

SiCN nanomechanical resonators for array-based biosensor applications

Csaba Guthy^{*,**}, Amit Singh^{*,**}, Jamshid Tanha^{***} and Stephane Evoy^{*,**}

*Department of Electrical and Computer Engineering, University of Alberta,
Edmonton, Alberta, T6G 2V4, Canada

**National Institute for Nanotechnology, Edmonton, Alberta, T6G 2M9, Canada

***Institute of Biological Sciences, Ottawa, ON, K1A 0R6, Canada

ABSTRACT

We report the high-yield fabrication of SiCN doubly-clamped nanomechanical resonator arrays for the specific detection of proteins. As a proof of concept, specific detection of Protein A has been demonstrated. The resonant frequencies of the individual resonators were determined using optical interferometry. The bare resonators displayed resonance frequencies of ~ 17 MHz. Immobilization of single domain antibody fragments resulted in frequency downshifts of ~ 341 kHz due to the added mass. Attachment of protein A yielded a further reduction of frequency by ~ 216 kHz. A much smaller frequency reduction of ~ 54 kHz was observed when the resonators are exposed to an identical solution containing no protein A.

Keywords: nanomechanical resonators, protein detection, NEMS, interferometry

1 INTRODUCTION

Rapid, sensitive and inexpensive analysis of biological molecules is of great importance to many biomedical applications, such as disease detection and monitoring, drug discovery, detection of pathogens, etc. Mechanical resonators have been demonstrated as highly sensitive

transducers for the detection of molecular systems as their mass sensitivity scales favorably as the dimensions are reduced. Zeptogram level mass sensitivities [1] have recently been demonstrated with nanowire based sensors. However, the main drawback of such bottom up approaches is the loss of precise control over device placement.

We have recently reported the development of a novel SiCN material of tunable mechanical properties for the fabrication of nanomechanical resonators [2] and the development of a fresh approach [3] to surface machining of suspended nanostructures that employs a combination of surface and bulk machining techniques. This approach produces resonators with very small undercuts of < 50 nm, thus significantly reducing clamping losses. The structures can also be suspended several microns above the surface regardless of their length, and are thus not subjected to stiction even without the use of critical point drying. This feature is of great importance for applications requiring repeated immersion in liquids. The unique properties of this SiCN material and the novel fabrication approach have now allowed the realization of arrays of suspended resonators as narrow as ~ 16 nm with a yield approaching 100 % (Fig 1.). The high yield and the small dimensions would allow for integration of such nanoresonators into large arrays for the multiplexed analysis of complex bimolecular mixtures.

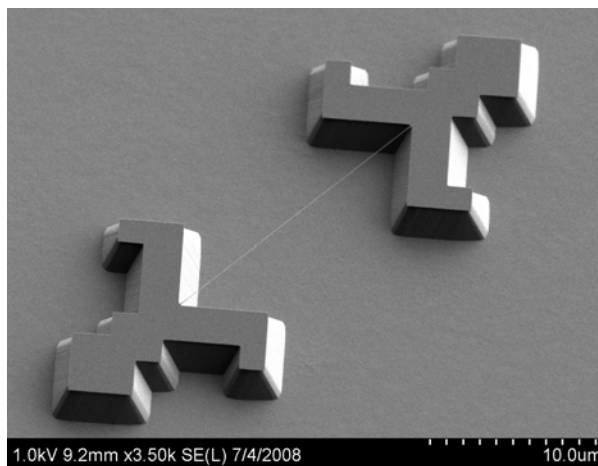
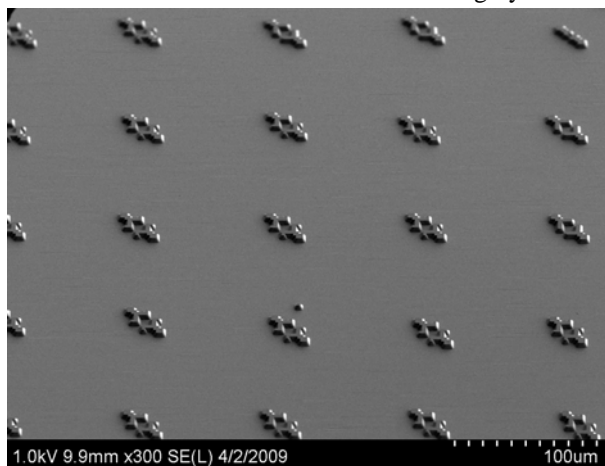


Figure 1. Left: SEM image of a 5x5 array of doubly-clamped 16 nm wide nanomechanical resonators. Right: Close-up image of a 16 nm wide and 24 um long nanomechanical resonator.

2 EXPERIMENTAL

A 50 nm thick SiCN layer was deposited by plasma-enhanced chemical vapor deposition (PECVD) onto single-crystal (100) silicon wafers (500 μm -thick, 100 mm-diameter). The SiCN-coated wafers were then annealed in a tube furnace at 500 C for 6 hours which resulted in a tensile stress of ~ 100 MPa. Next, the resonator beams and the supporting pads were patterned using electron beam lithography (Raith 150). A 30 nm thick Cr film, deposited by thermal evaporation and subsequently lifted off in acetone, was used as a mask for reactive ion etching. Finally, the resonators were released by anisotropic etch in KOH solution (35%) saturated with IPA. Figure 1 (right image) shows SEM of a typical 16 nm wide 50 nm thick and 14 μm long SiCN resonators.

The experimental setup is illustrated in Figure 2. The chips were mounted onto a piezoelectric element which was actuated by the tracking output of a spectrum analyzer (Agilent model 4411B). The beam of a laser diode ($\lambda = 655$ nm) was directed through a beamsplitter and focused onto the substrate using a NA=0.45 microscope objective. At resonance, motion of the nanoresonators relative to the substrate created a moving fringe pattern that was reflected back through the microscope objective, was redirected by the beamsplitter, and impinged on an AC coupled photodetector (New Focus model 1601).

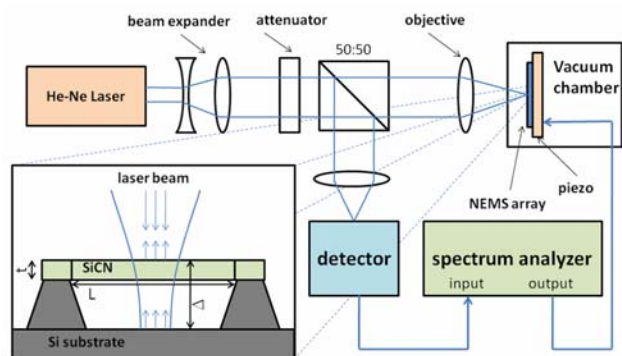


Figure 2. Schematic diagram of the interferometric setup. The resonator chips are attached to a piezoelectric element mounted inside a vacuum chamber. The element is actuated from the output signal of a Hewlett Packard ESA-L1500A spectrum analyzer. A He-Ne laser ($\lambda = 633$ nm) is focused onto the resonator using a 0.45 NA microscope objective to a beam spot size of ~ 5 μm . The inset (left lower corner) illustrates the interference of the focused laser beam that is partially reflected from the substrate and from the resonator. The modulated signal is reflected back through the microscope objective. A beam splitter diverts the reflected signal towards a New Focus 1601 AC coupled photodetector, whose output is fed into the input of the spectrum analyzer.

3 RESULTS AND DISCUSSION

In order to utilize such SiCN nanoresonators for the specific detection of various analytes, analyte-specific functional layers need to be immobilized onto their surface. The binding affinity of these layers is then assessed by monitoring the resonant frequency shifts related to any added mass on each individual device. As a model target system we chose to demonstrate the specific detection of protein-A using single domain antibody fragments (sdAb). Immobilization of antibody fragments onto array I results in consistent resonant frequency downshifts of ~ 341 kHz. The frequencies further downshift by ~ 216 kHz due to protein A attachment (Fig. 2).

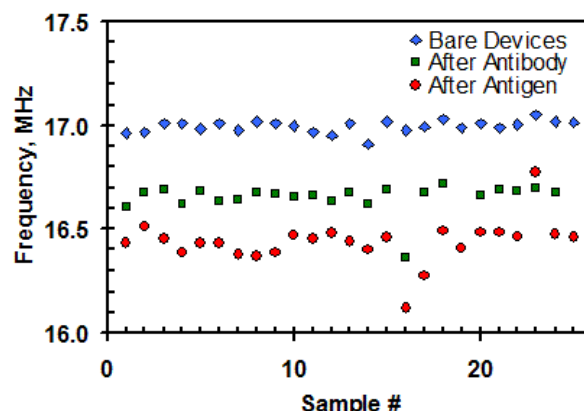


Figure 3. Resonant frequencies of the 25 individual resonators of Array I. The blue diamonds designate the individual device frequencies of the bare resonators.

Immobilization of antibodies results in frequency downshifts of ~ 341 kHz (green squares). Capture of protein A further downshifts the frequencies by ~ 216 kHz (red circles).

Another “negative control” array II (Fig. 3) was processed identically except protein-A was not added to the solution. The frequency shifts due to this “solvent only” step are much smaller (~ 54 kHz), further supporting that the significant frequency downshifts in array I are indeed due to protein-A capture.

We are currently scaling up our fabrication methodology to produce large sensor arrays containing millions of individual devices per square centimeter. Our eventual goal is to use such large arrays of such devices for the detection and analysis of disease biomarkers, including but not limited to multiple sclerosis and cancer biomarkers.

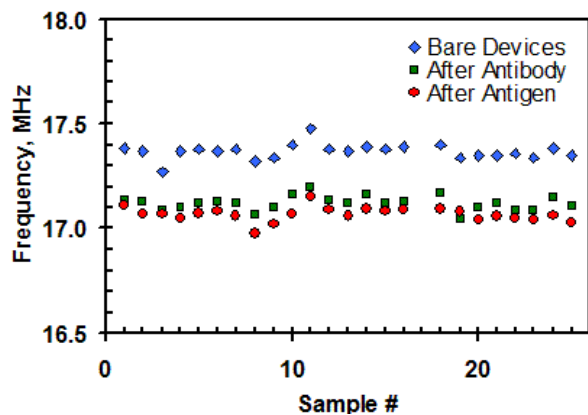


Figure 4. Resonant frequencies of Array II. This “negative control” array was processed identically except protein A was not added to the solution in the detection step. Similarly to Array I, immobilization of antibodies results in $\Delta f \sim 248$ kHz. The second “solvent only” step results in much smaller frequency downshifts of ~ 54 kHz.

REFERENCES

- [1] Y.T. Yang, C. Callegari, X.L. Feng, K.L. Ekinici and M.L. Roukes, *Nano Lett.* 6, 583, 2006.
- [2] L.M. Fischer, N. Wilding, M. Gel, S. Evoy, *J. of Vacuum Science & Technology B* 25, 33, 2007.
- [3] L.M. Fischer, V.A. Wright, C. Guthy, N. Yang, M.T. McDermott, J.M. Buriak and S. Evoy, *Sens. Actuators B* 134, 613, 2008.